

Design and Development of a Test Facility to Study Two-Phase Steam/Water Flow
in Porous Media

Ashok K. Verma, Karsten Pruess, G. S. Bodvarsson,
C. F. Tsang and Paul A. Witherspoon

Lawrence Berkeley Laboratory
University of California
1 Cyclotron Road
Berkeley, CA, 94720

INTRODUCTION

The concept of relative permeability is the key concept in extending Darcy's law for single phase flow through porous media to the two-phase flow regime. Relative permeability functions are needed for simulation studies of two-phase geothermal reservoirs. These are poorly known inspite of considerable theoretical and experimental investigations during the last decade. Since no conclusive results exist, many investigators use ad hoc parameterization, or adopt results obtained from flow of oil and gas (Corey, 1954). It has been shown by Reda and Eaton (1980) that this can lead to serious deficiencies. Sensitivity of the relative permeability curves for prediction of mass flow rate and flowing enthalpy into geothermal wells has been studied by many investigators (eg. Eaton and Reda (1980), Bodvarsson et al (1980), Sun and Ershagi (1979) etc.) It can be concluded from these studies that the behavior of a two-phase steam/water reservoir depends greatly on the relative permeability curves used. Hence, there exists a need for obtaining reliable relative permeability functions.

The approach taken at Lawrence Berkeley Laboratory to obtain relative permeability curves and their dependence on fluid and matrix properties is summarized in Fig. 1. Thermo-dynamic studies are carried out to develop the equations governing two-phase steam/water flow in porous media and to analyze the relationship between mass flow rate and flowing enthalpy. These relationships will be verified against experimental results and subsequently will be used to develop a field analysis technique to obtain in-situ relative permeability parameters. Currently our effort is concentrated on thermo-dynamic analysis and development of an experimental facility. This paper presents some of the findings of our theoretical work and also describes the design and development effort for the experimental facility.

In the first part of this paper we present some basic theoretical studies of the mechanism of phase trapping and the effect of pore geometry on the relative permeability functions. The flow conditions which may support phase trapping are identified and it is recommended that these operating conditions be avoided

during the experiment. The effect of pore geometry on the relative permeability functions is studied by considering two different flow configurations, a circular tube and a plane fracture.

In the second part of this paper a description of the experimental setup is given. The proposed experimental setup is similar to that of Reda and Eaton (1981). However, a significant improvement in the analysis of the operating conditions is achieved by considering the effects of capillary pressure and the end effects resulting from it. We also propose to use a capillary pressure probe to obtain the dependence of capillary pressure on saturation under dynamic conditions.

PREVIOUS WORK

Various investigators have attempted to determine the relative permeability curves for steam/water flow in porous media. Experimental works to determine the relative permeability curves have been reported, among others, by Corey (1954), Chen et. al (1978), and Counsil and Ramey (1979). Grant (1977), Horne and Ramey (1978) and Shinohara (1978) used flow rate and enthalpy data from the Wairaki geothermal field in New Zealand to obtain information about in-situ relative permeability functions. A completely theoretical model was proposed by Menzies (1982), and Gudmundsson et al (1983), who used a streamtube model to obtain relative permeability functions.

BASIC STUDIES

In this section we study the mechanism of phase trapping and the effect of pore geometry on the relative permeability functions.

Phase Trapping

Phase trapping can occur when one of the phases becomes immobile under the action of capillary pressure in a channel full of the other phase which flows around it. Both water and steam can be trapped in flow channels when the thermodynamic conditions are such that the net rate of phase transformation, at the interface of the trapped phase and the flowing phase, equals zero. This phenomenon is important in this study because of two reasons:

- (i) phase trapping is an important mechanism of permeability reduction
- (ii) phase trapping can lead to local changes that are hysteretic in nature. (Observed by Udell (1983) in his "Hot Wire" experiment).

To study the phase trapping mechanism in a two-phase steam/water flow in porous media, the following assumptions are made:

- a) flow is one dimensional and horizontal
- b) water is the wetting fluid. Steam resides on the concave side of the steam/water interface and both the liquid and the steam phases are superheated (Udell, 1983)
- c) pores are large enough so that the effect of adsorption on phase equilibrium can be neglected
- d) water, vapor and the matrix are locally in thermodynamic equilibrium and any phase transformation is quasistatic.

With these assumptions we can show that, (see appendix-I)

- i) the vapor phase can be trapped when liquid is flowing in the direction of increasing temperature
- ii) the liquid phase can be trapped if vapor is flowing in the direction of decreasing temperature and also

$$\frac{\partial}{\partial x} \left(\frac{T}{P_c} \right) < 0$$

This indicates that relative permeability of a phase may depend not just on saturation but also on the local temperature gradient.

Effect of pore geometry

To study the effect of pore geometry on relative permeability functions we use an approach similar to that of Yuster (1951). The two different flow channel geometries considered are (i) a circular tube, and (ii) a plane fracture.

In both these cases the flow is assumed to be separated with water being the wetting fluid. We also assume that the surface temperature distribution is such that no flashing or condensation can occur. Under these conditions, the relative permeability functions for the circular tubes are (Yuster, 1951)

$$k_{rw} = (1 - S_v)^2 \quad (1)$$

$$k_{rv} = 2 S_v \frac{\mu_v}{\mu_w} + S_v^2 \left(1 - 2 \frac{\mu_v}{\mu_w} \right) \quad (2)$$

Following the same line of reasoning we can show that for plane fractures

$$k_{rw} = 1 - 1.5 S_v + 0.5 S_v^3 \quad (3)$$

and

$$k_{rv} = 1.5 \frac{\mu_v}{\mu_w} S_v - S_v^3 \left(1.5 \frac{\mu_v}{\mu_w} - 1 \right) \quad (4)$$

A plot of these relative permeability curves, for

$$\frac{\mu_v}{\mu_w} = 0.4 \text{ and } 0.1,$$

is shown in Fig. 2. From these curves we can see that for a given saturation the parallel plate configuration has a higher relative permeability for the water phase than the circular tube model. However, the vapor phase relative permeability has the opposite trend. This phenomenon occurs because for a given saturation the parallel plate configuration will have a thicker water layer than the circular tube model.

It is easy to show from equations 1-4 that in the two-phase zone (i.e. $0 < S_v < 1$) the sum of relative permeabilities is less than one (i.e. $k_{rw} + k_{rv} < 1$) as long as the viscosity ratio (μ_v/μ_w) remains less than unity.

However, this model is rather simplistic and further studies are needed in which effects of phase transformation should be included.

PROPOSED EXPERIMENTAL SETUP AND OPERATING CONDITIONS

The proposed experimental setup (Fig.3) is similar to that of Reda and Eaton (1981). The test sample is a sand pack in a glass cylinder (3" I.D. x 36" length), mounted vertically to avoid the problem of flow stratification. The outer surfaces of this cylinder are made adiabatic with the aid of computer controlled guard heaters. Liquid water at constant temperature is pumped into the inlet end of the test sample at a constant flow rate with the aid of a dual-cylinder, constant-flow rate, metering pump.

Electric heaters are installed inside the porous matrix at the inlet end. A controlled amount of power is supplied to these heaters through a stabilized power supply to cause boiling and the power input is adjusted to achieve the required flow quality. The mixture of steam and water leaves the test sample through an exit chamber designed to reduce the end effects. The exit end is maintained at constant pressure with the aid of a back pressure regulator.

Pressure, temperature, capillary pressure and saturation readings will be taken at regular intervals in the central portion of the test column. Saturation readings will be taken with the aid of a γ -ray densitometer, which avoids disturbing the flow while taking readings.

Desirable operating conditions have been studied with the aid of numerical modeling. It was speculated that the effect of capillary pressure, and the end effects resulting from it, would be very significant. To study these effects, various capillary pressure curves were incorporated in a numerical code MULKOM (Pruess, 1983), and test runs were simulated. A typical result of a simulation with the end effects is shown in Fig. 4 and for the purpose of comparison, a typical result without the end effect is shown in Fig. 5. From these figures we can see that, while the four parameters of interest, P_v , P_c , T and S_v , vary monotonically with more or less constant gradient in Fig. 5, the end effects cause a very sharp gradient of P_v , P_c and S_v (Fig. 4) over the last 20 cm of the test column near the exit end. This phenomenon occurs because of the physical nature of the problem which requires that the capillary pressure must equal zero at the exit.

We have also considered the effects of matrix properties, boundary conditions and the relative permeability functions on the proposed experiment. Results of simulations using many parameter combinations show that it is possible to obtain a region of almost constant saturation over an extended length of the test column. Readings taken in this region can be analyzed to yield relative permeabilities without much difficulty.

The analysis technique follows that of Reda and Eaton (1981). By considering the conservation of mass and energy in a two-phase concurrent flow in a vertical test section, we derive the following relationships.

$$f = \frac{m_o (h_o - h_w) - m_o g z + q_o - q}{m_o (h_v - h_w)} \quad (5)$$

$$k_{rw} = \frac{(f - 1) m_o \mu_w v_w}{kA \frac{d}{dz} (P_w + \rho_w g z)} \quad (6)$$

$$k_{rv} = - \frac{f m_o \mu_v P_v}{kA \frac{dP_v}{dz}} \quad (7)$$

The right hand side of equations 5-7 consists of quantities which are either known or can be measured from the experiment and hence equations 6 and 7 can be used to calculate the relative permeabilities.

SUMMARY

Criteria for phase trapping in flow channels have been developed based on the thermodynamics of curved interfaces. It is shown that the vapor phase can be trapped if liquid is flowing in the direction of higher temperature. On the other hand, liquid can be trapped if vapor is flowing in the direction of lower temperature. Based on an ideal capillary analysis we conclude that the shape of the relative permeability functions depend on the pore geometry and the viscosity ratio of steam and water. We also show that the sum of

the relative permeabilities in the two-phase zone is generally less than unity. Our analysis neglects phase change, and a more realistic treatment of steam-water flow is needed before conclusive results can be obtained. From the basic studies we conclude that the relative permeability functions may depend, among other parameters, on the fluid properties, pore geometry and flow conditions.

Results of the numerical studies show that the end effects can be very significant. However, it is possible to design and experiment such that a nearly constant vapor saturation region exists over an extended portion of the test sample. In this region, the capillary pressure gradient is small and thus the experimental data can be easily interpreted.

NOMENCLATURE

A	core cross-sectional area
f	dynamic quality ($m_v/(m_v + m_w)$)
g	acceleration of gravity
h	specific enthalpy
k	intrinsic permeability of the sample
k_r	relative permeability
m	mass flow rate
P	Pressure
q	heat flux due to conduction
R	gas constant for vapor
r_{eq}	equivalent radius of curvature $r_{eq} = 2\gamma/\rho_c$
S	inplace saturation
T	temperature
v	specific volume
x	linear distance
z	vertical distance along the core holder
μ	absolute viscosity
γ	Gibb's free energy per unit area of interface

SUBSCRIPTS

c	capillary
o	condition at the inlet of the test sample
v	vapor phase
w	water phase
∞	infinite radius of curvature

ACKNOWLEDGEMENT

This work was supported by the Assistant Secretary for Conservation and Renewable Energy, Office of Renewal Technology, Division of Geothermal and Hydropower Technologies of the U.S. Department of Energy under Contract No. DE-AC03-76SF00098.

REFERENCES

Bodvarsson, G.S., O'Sullivan, M.J. and Tsang, C.F., 1980, "The Sensitivity of Geothermal Reservoir Behavior to Relative Permeability Parameters", Proc. 6th Workshop Geothermal Res. Eng., Stanford.

Chen, H.K., Counsil, J.R., and Ramey, H.J., 1978, "Experimental Steam-water Relative Permeability Curves", Trans. Geothermal Resources Council, Vol. 2, 102-104.

Corey, A.T., 1954, "The Interrelation Between Gas and Oil Relative Permeabilities", Prod. Mon., 19, 38-41.

Counsil, J.R., and Ramey, H.J., 1979, "Drainage Relative Permeabilities Obtained from Steam-Water Boiling - Flow and External Gas Drive Experiments", Transactions, Geothermal Resources Council, Vol. 3, 141-143.

Grant, M.A., 1977, "Permeability Reduction Factors at Wairaki," Paper presented at AIChE-ASME Heat Transfer Conference, AIChE, Salt Lake City, Utah, Aug. 15-17.

Gundmundsson, J.S., Menzies, A. J., and Horne, R. N., 1983, "Streamtube Relative Permeability Functions for Flashing Steam-Water Flow in Fractures", SPE Paper No. 11686 presented at the California Regional Meeting of the SPE, Ventura.

Horne, R.N. and Ramey, H.J., 1978, "Steam/water Relative Permeability From Production Data", Transactions, Geothermal Research Council, Vol. 2, 291-293.

Menzies, A.J., 1982, "Flow Characteristics and Relative Permeability Functions for Two-Phase Geothermal Reservoirs from a One-Dimensional Thermodynamic Model", M.S. Report, Stanford University.

Pruess, K., 1983, "Development of the General Purpose Simulator MULKOM," Annual Report 1982, Earth Sciences Division, Lawrence Berkeley Laboratory, Berkeley, CA.

Reda, D.C. and Eaton, R.R., 1980, "Influence of Steam/Water Relative Permeability Models on Predicted Geothermal Reservoir Performance: A Sensitivity Study", 6th Annual Workshop on Geothermal Reservoir Engineering, Stanford, Dec. 15-18.

Reda, D.C. and Eaton, R.R., 1981, "Definition of a Facility for Experimental Studies of Two-Phase Flows and Heat Transfer in Porous Materials", AIAA 16th Thermophysics Conference, Paper No. AIAA-81-1190.

Shinohara, K., 1978, "Calculations and Use of Steam/Water Relative Permeabilities in Geothermal Reservoirs," M.S. Report, Stanford University.

Sun, H. and Ershaghi, I., 1979, "The Influence of Steam-Water Relative Permeability Curves on the Numerical Results of Liquid Dominated Geothermal Reservoirs", Transaction, Geothermal Resources Council, Vol. 3, 697-700.

Udell, K., 1983, "Heat Transfer in Porous Media Heated from Above with Evaporation, Condensation and Capillary Effects", Journal of Heat Transfer, Aug. 1983, 485-492.

Yuster, S.T., 1951, "Theoretical Considerations of Multiphase Flow in Idealized Capillary Systems", Proc. 3rd World Petroleum Congress.

APPENDIX

Mechanism of phase trapping in flow channels.

The required thermodynamic relations are:
Laplace's equation

$$P_c = P_v - P_w = 2\gamma/r_{eq}, \text{ and} \quad A.1$$

Kelvin's equation

$$RT \ln(P_v/P_\infty) = \frac{v_w \gamma}{r_{eq}} \quad A.2$$

First we apply these to a trapped vapor bubble in a channel full of flowing water (Fig. 6). Considering a horizontal flow,

$$\frac{\partial P_w}{\partial x} < 0 \quad A.3$$

Since the vapor bubble does not flow it must have constant pressure throughout (i.e. $P_v = \text{const. inside the bubble}$). Therefore

$$\frac{\partial P_c}{\partial x} = -\frac{\partial P_w}{\partial x} = -\frac{2\gamma}{r_{eq}^2} \frac{\partial r_{eq}}{\partial x} \quad A.4$$

Assuming that the vapor phase and the liquid phase are in thermodynamic equilibrium along their interface, the temperature gradient is obtained by differentiating eqn. A.2

$$\frac{\partial T}{\partial x} = - \left[\frac{v_w \gamma}{R \ln(P_\infty/P_v) r_{eq}^2} \right] \frac{\partial r_{eq}}{\partial x} \quad A.5$$

In the assumed configuration the vapor is superheated and hence $P_\infty > P_v$. Therefore the quantity in the square bracket in eqn. A.5 is positive.

Considering eqns. A.3, A.4 and A.5 it can be concluded that for the mechanical and thermodynamic equilibrium of the trapped vapor bubble

$$\frac{\partial r_{eq}}{\partial x} < 0 \quad A.6$$

$$\frac{\partial T}{\partial x} > 0 \quad A.7$$

Now we consider trapping of liquid phase in a flow channel (Fig. 7). In the trapped section liquid has constant pressure (i.e. $P_w = \text{constant}$). For mechanical equilibrium, eqn. A.1 yields

$$\frac{\partial P_c}{\partial x} = \frac{P_v}{\partial x} = - \frac{2\gamma}{r_{eq}^2} \frac{\partial r_{eq}}{\partial x} \quad A.8$$

Since

$$\frac{\partial P_c}{\partial x} < 0$$

we must have $\frac{\partial r_{eq}}{\partial x} > 0$

Considering the thermodynamic equilibrium of the phases along the interface, eqn. A.2 yields

$$\frac{1}{P_v} \frac{\partial P_v}{\partial x} = \frac{\gamma v_w}{RT^2 r_{eq}^2} \frac{\partial (T r_{eq})}{\partial x} \quad A.9$$

Since

$$\frac{\partial P_v}{\partial x} < 0$$

equations A.8 and A.9 yield that for mechanical and thermodynamic equilibrium of the trapped liquid phase T and r_{eq} must satisfy

$$\frac{\partial (T r_{eq})}{\partial x} < 0 \quad A.10$$

or

$$r_{eq} \frac{\partial T}{\partial x} < - T \frac{\partial r_{eq}}{\partial x}$$

Incorporating the eqn. A.8

$$\frac{\partial T}{\partial x} < 0 \quad A.11$$

From eqn. A.1, A.10 and A.11

$$\frac{\partial}{\partial x} \left(\frac{T}{P_c} \right) < 0 \quad A.12$$

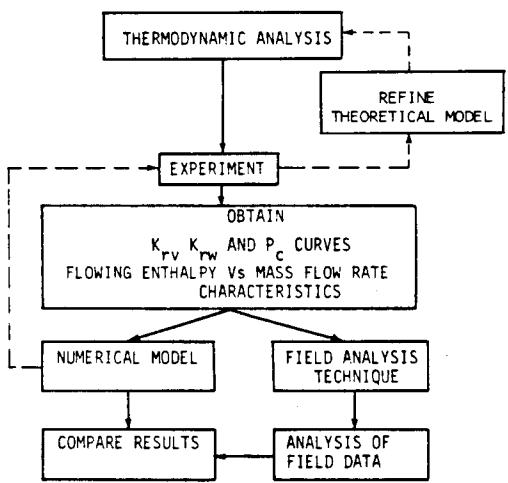


Fig. 1. Overall approach to determination of relative permeability functions for steam/water flow.

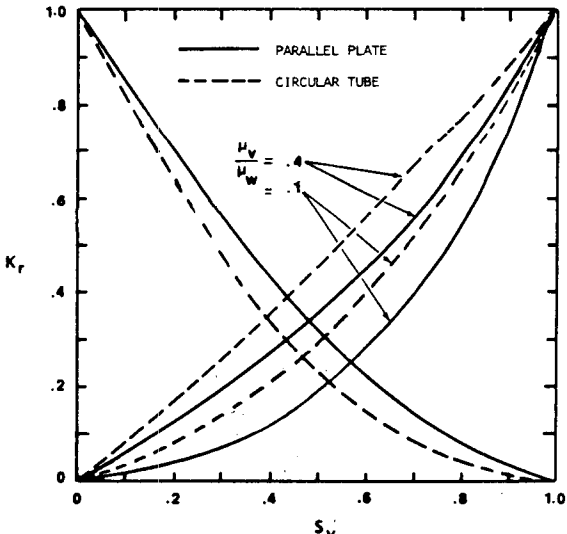


Fig. 2. Relative permeability curves for idealized capillary tubes.

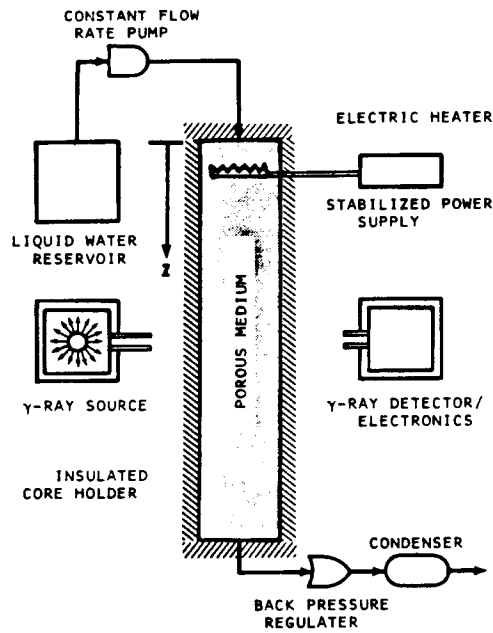


Fig. 3. Schematic of the experimental setup.

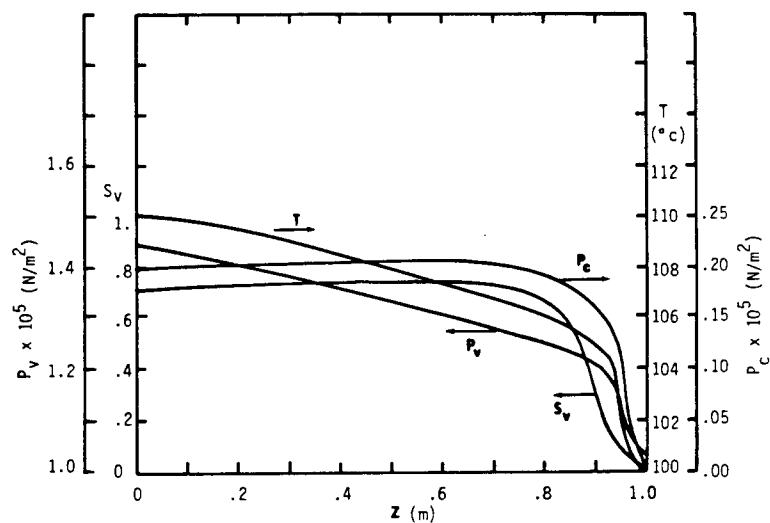


Fig. 4. Simulated test results with the end effects.

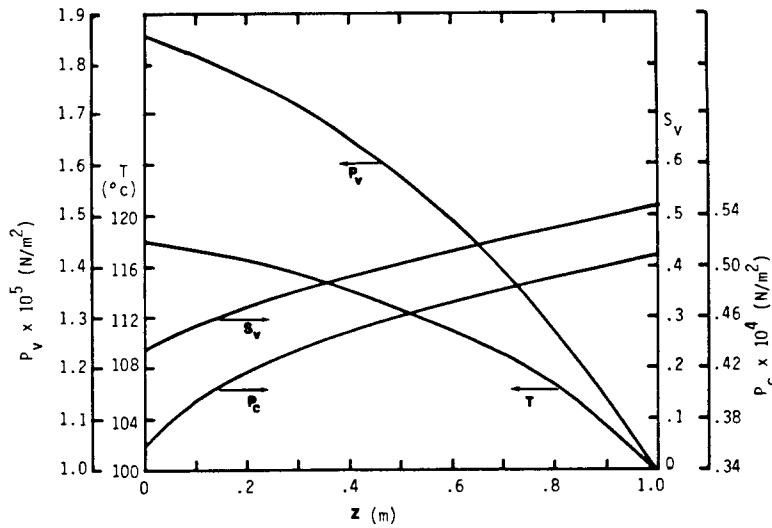


Fig. 5. Simulated test results without the end effects.

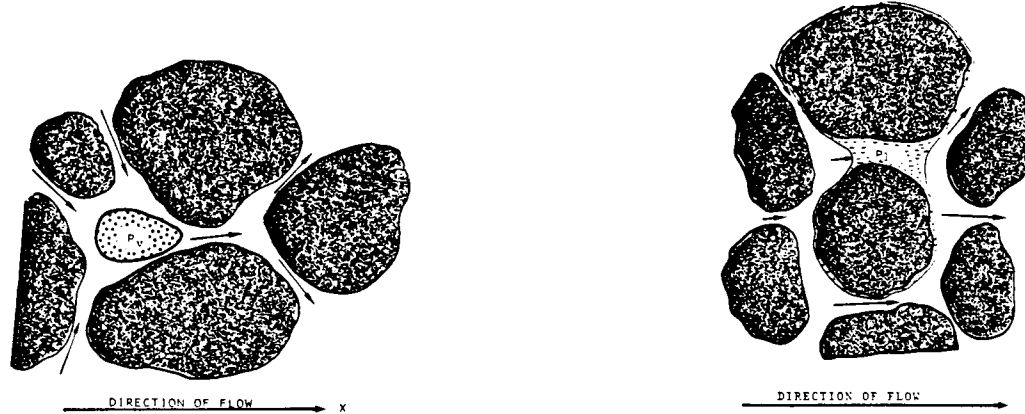


Fig. 6. Vapor trapping in a flow channel.

Fig. 7. Liquid trapping in a flow channel.